Synthesis and optical properties of zinc oxide/carbon quantum dots nanocomposites

SEDIGHE ZAHERI[1], HAMID AKHERAT DOOST[2*], EHSAN KOUSHKI[3] AND REZA TAYEBEE[1]

[1]Department of Chemistry, Faculty of Sciences, Hakim Sabzevari University, Sabzevar, 96179-76487, Iran
[2]Department of Physics, Central Tehran Branch, Islamic Azad University, Tehran 14696-69191, Iran
[1]Department of Physics, Faculty of Sciences, Hakim Sabzevari University, Sabzevar, 96179-76487, Iran

Commented [a1]: Please include your fax and phone numbers

Abstract

Due to their special properties and applications, Nanoparticles have received a lot of attention and attracted researchers. Meanwhile, zinc oxide nanoparticles have excellent transparency, electrical, and optical properties. In this research, nanoparticles were synthesized using the hydrothermal method, and a ZnO-CQDs/PVA nanocomposite was prepared using the injection method into a polymer substrate. Optical and structural properties were investigated by various methods such as TEM, XRD, UV-VIS, and DLS. The energy gap in quantum dot zinc oxide-carbon nanocomposite with concentrations of 1240, 2840, and 3720 micrograms injected into the polymer solution was calculated as 3.38, 3.39, and 3.4 eV, respectively. The results show that the energy gap increases with the increase in carbon quantum dots in the nanocomposite indicating the effect of the Burstein-Moss phenomenon. This phenomenon means an increase in the energy gap in semiconductor materials, which can improve the performance of nanoelectronic and optical materials.

Keywords

Energy gap
Nanomaterial synthesis
Zinc oxide/carbon quantum dots nanocomposites

---

*Corresponding author: Hamid Akherat Doost

Assistant Professor of Laser Photonics; Ph.D., Department of Physics,

Faculty of Basic Sciences, Central Tehran Branch, Islamic Azad University, Tehran, Iran

Post Code: 14696-69191

Tel: (++98)-21-44600196

Email1: hamidakherat@gmail.com

E-mail2: ha.akherat@iau.ac.ir

1. Introduction

Zinc oxide is an important semiconductor characterized by a band gap of 3.37 eV and a high excitation energy of 60 meV at room temperature (Xu et al., 2018). It is a typical n-type semiconductor that belongs to group II-VI (Onodera and Takes, 2012). In recent years, zinc oxide has garnered considerable attention due to its unique optical, electronic, and piezoelectric properties, as well as its potential applications in solar cells, blue light-emitting diodes, sensors, and attenuators (Jalili et al., 2023). Zinc oxide is utilized in various high-tech devices, including those for generating sound waves, serving as transparent conductive electrodes in solar cells, and in electroluminescent screens, electromechanical and optoelectronic devices, filter-separating coupled waveguides,

thermal mirrors, photothermal multilayers, and gas sensors (Aranovich et al., 1980; Nanto et al., 1993; Chang et al., 1995; Bacaksiz et al., 2008; Zhang and Li, 2009; Koushki et al., 2011; Baedi et al., 2021; Khaled and Berardi, 2021; Al Ja'farawy et al., 2022; Liu et al., 2023).

Zinc oxide has four notable defects, including:

1) Defects in the Zinc Lattice
2) Oxygen Vacancies
3) The replacement of oxygen atoms with elements that possess lower valence.
4) The replacement of zinc atoms with a metal that has a higher valence results in an intrinsic semiconductor (Gao et al., 2021). This material is widely utilized in various optoelectronic and electronic applications due to its large exciton binding energy and wide direct bandgap. The extensive bandgap enables it to endure high electric fields, achieve a high breakdown voltage, and generate low noise (Alim et al., 2006).In general, zinc oxide exhibits two types of emissions: one in the ultraviolet region, associated with near-band edge emission, and the other in the visible region, linked to broad band emission resulting from deep levels within the band gap. This emission occurs within the wavelength range of 410 to 730 nm. In the visible spectrum, the natural width of the emission typically comprises a combination of multiple emissions.

The observed emission in the visible region is associated with the intrinsic defects of the zinc oxide network, although the exact origin of these defects remains uncertain. One of the challenges in identifying the source of band defects in zinc oxide is that the bands are broad and overlapping. The emission in the ultraviolet region is attributed to the recombination of free excitons, which occurs as a result of exciton-exciton collisions.

Zinc oxide possesses deep levels that can be categorized into internal and external deep levels. Internal deep levels arise from defects such as oxygen interstitials, oxygen vacancies, and zinc vacancies. The method of synthesis and the concentration of materials also influence the inherent defects present in zinc oxide. When a defect is ionized at room temperature, it can lead to the formation of a surface transition. Conversely, if the defect remains un-ionized, it is referred to as a deep transition level. In terms of conductivity, zinc oxide is considered one of the most effective materials for applications in vacuum fluorescent display screens and field emission displays (Hartnagel, 1995).The optical properties of zinc oxide are strongly influenced by its binding energy structure and lattice dynamics. Zinc oxide is a transparent material with a cutoff wavelength in the ultraviolet region, specifically related to wavelengths shorter than 400 nm (Sarkar et al., 1991). This characteristic allows for the transmission of visible light while absorbing ultraviolet rays, which is one of the practical applications of zinc oxide.

In the visible spectrum, zinc oxide can transmit up to 90% of light when properly prepared. Zinc oxide can be doped with various elements from the periodic table, which enhances its optical and electrical properties. Research has shown that the energy gap in doped materials exhibits a linear relationship with the density of charge carriers (N) (Burstein et al., 1954).

The energy gap of zinc oxide layers may exhibit a linear relationship with $N^{2/3}$, which can be explained by the full Burstein-Moss model (Berggren and Martino, 1971).

In addition, other studies indicate that when the impurity level is high—specifically, when the charge density increases around a certain threshold (the state in which charge carriers become so abundant that the semiconductor transitions to a conductor)—the energy gap exhibits a linear relationship with $N^{1/3}$ (Mahan, 1980; Chang et al., 2003).

Nano carbon quantum dots are a novel class of materials primarily recognized for their fluorescence capabilities. These nanoparticles have garnered significant attention from researchers due to their straightforward availability and ease of synthesis. Key properties include water solubility, chemical inertness, ease of functionalization, optical brightness, low toxicity, biocompatibility, and resistance to photobleaching. These attributes have established carbon quantum dots as essential components in optics, solar technology, and photocatalysis.

Carbon quantum dots exhibit broad emission spectra that span visible, ultraviolet, and near-infrared wavelengths, resembling the emission capabilities of semiconductor quantum dots. This versatility underscores their potential for diverse applications and highlights their significance in contemporary nanotechnology research (Willander et al., 2010).

Research on carbon nanomaterials is still in its early stages (Majles Ara et al., 2015). The discovery of carbon quantum dots was accidental, much like many other scientific breakthroughs. These quasi-spherical nanoparticles

were first unintentionally produced in 2004 during the electrophoretic purification of single-walled carbon nanotubes. Initially identified as fluorescent particles, they were separated from carbon impurities during the synthesis of carbon nanotubes using the electric arc method.

Since their discovery, research in this field has expanded significantly. Scientists have developed various synthesis methods for carbon quantum dots, leading to substantial advancements in understanding their physical and chemical properties, particularly the origins of their inherent fluorescence. It has been established that the fluorescence intensity of these materials correlates with their surface characteristics, highlighting the importance of surface modifications in enhancing their optical properties (Li et al., 2012). Semi-spherical carbon quantum dots typically have diameters below 10 nm. While some hollow structures of carbon quantum dots have been reported, they generally exist as nanocrystals or amorphous structures containing sp^2 carbon clusters. Carbon quantum dots are essentially planar graphite lattices with carbon-carbon bond lengths influenced by the presence of functional groups, typically ranging from 0.18 to 0.24 nanometers. The interlayer distance in these structures is approximately 0.334 nanometers, but this can vary depending on synthetic methods, surface modifications, and the types of atoms and functional groups present. These factors significantly impact the structure, as well as the physical and chemical properties, of carbon quantum dots (Willander et al., 2010).

Carbon quantum dots exhibit strong absorption of short-wavelength photons primarily due to π-π^* transitions arising from C=C double bonds. Typically, these nanoparticles absorb strongly in the range of 260 to 300 nm, extending into the visible spectrum. The absorption characteristics can be modulated by the presence of functional groups and surface modifications (Zhao et al., 2008).

An appealing feature of carbon quantum dots is their tunable fluorescence, driven by quantum effects. However, their quantum efficiency is typically low, often below 10%. Surface roughness plays a crucial role in enhancing fluorescence, with the fluorescence intensity being more dependent on surface characteristics rather than the carbon sp^2 clusters in the core structure.

After synthesis, carbon quantum dots can emit light ranging from blue to green, and occasionally red, under ultraviolet light excitation. This emission behavior underscores their potential applications in various fields, particularly in optoelectronics and biomedical imaging.

The fluorescence observed in carbon quantum dots is believed to originate from the recombination of electrons and holes confined to their surface. This phenomenon suggests that the fluorescence of these materials can be influenced or quenched by electron donor and acceptor materials. Therefore, the optical properties of carbon quantum dots are characterized by the competition between radiative (fluorescent) and non-radiative (non-fluorescent) processes occurring on their surfaces (Jia et al., 2012; Wang et al., 2013).

Another important optical property of carbon quantum dots is their ability for multi-photon excitation. This property allows them to emit shorter wavelength light when they absorb two or more longer wavelength photons simultaneously. This feature is particularly advantageous for applications such as in vivo imaging, where longer wavelengths (like near-infrared) can penetrate deep tissues effectively. The low background interference and low photon-induced toxicity associated with this imaging method make carbon quantum dots suitable for high-resolution molecular imaging applications (Liu et al., 2012).

2. Experimental

Metal oxide nanocomposites and carbon quantum dots have numerous applications in the fields of photocatalysis, optics, and photoluminescence. Below, we will explore these applications in detail:

2.1. Photocatalytic

Metal oxide nanocomposites and carbon quantum dots are utilized as photochemical catalysts. In this application, light photons energize electrons, activating various chemical processes involving these nanocomposites. These processes include the decomposition of water into hydrogen and oxygen, the production of hydrogen fuel, and the synthesis of organic compounds. Additional applications of photocatalysis encompass water and air purification, as well as energy production in solar cells.

2.2. Optical

Metal oxide nanocomposites and carbon quantum dots have a wide range of applications in optical fields. For instance, these nanocomposites can serve as optical sensors for detecting both organic and inorganic substances. Furthermore, they are utilized in the fabrication of optical chips and electroluminescent diodes.

2.3. Photoluminescence

Photoluminescence refers to the emission of light by a substance following the absorption of light. Due to their unique electronic properties, carbon quantum dots can absorb and emit light across various wavelengths. These characteristics render carbon quantum dots suitable for manufacturing electroluminescent diodes and optical display panels. Additionally, these nanocomposites are employed in the production of electroluminescent lamps and optical sensors.

In summary, metal oxide nanocomposites and carbon quantum dots represent innovative materials in the fields of photocatalysis, optics, and photoluminescence, providing new opportunities and advancements in these domains.

To synthesize ZnO nanoparticles (see Fig. 1), a solution of sodium acetate ($(CH_3COO)_2.2H_2O$, 0.1 M) in 50 mL of methanol and stirred. A zinc hydroxide ($Zn(OH)_2$) solution, with concentrations ranging from 0.2 to 0.5 M in NaOH and also prepared in methanol, was added gradually until the pH of the mixture reached between 8 and 11. The reaction mixture was stirred at room temperature for 24 hours to stabilize the nanoparticles.

To prepare carbon quantum dots (CQDs), a plate was cleaned with detergent, alcohol, and acetone using an ultrasonic cleaner for 8 minutes, then dried. Next, 5.0 g of citric acid was placed on the plate and heated on a heater-stirrer at 250 °C for 10 minutes. After heating, the plate was allowed to cool to room temperature for 15 minutes. This process was repeated two additional times, with the temperature increased to 300 °C during each iteration. This thermal treatment resulted in the successful preparation of carbon quantum dots.

To dope or synthesize quantum carbon and zinc oxide nanoparticles together, a specific amount of carbon quantum dots was dissolved in water and stirred for one hour under consistent conditions. This solution was then added to the previously prepared zinc oxide nanoparticles and stirred for an additional two hours.

If it was necessary to dope quantum carbon and zinc oxide nanoparticles in powder form, the solution was transferred to an autoclave and placed in an oven at 100 °C for 12 hours. Finally, the resulting solution was washed several times with methanol, centrifuged, and dried at room temperature to obtain the doped quantum carbon and zinc oxide nanoparticles in powder form.

In this method, the objective was to utilize zinc oxide nanoparticles at a consistent concentration while varying the concentrations of carbon quantum dots. Specifically:

1. Substance (1): The concentration of carbon quantum dots was 124×10^{-4} M.
2. Substance (2): The concentration of carbon quantum dots was 248×10^{-4} M.
3. Substance (3): The concentration of carbon quantum dots was 372×10^{-4} M.

These concentrations indicate the amount of carbon quantum dots used in each sample relative to an equivalent concentration of zinc oxide nanoparticles, resulting in varying doping levels for the nanocomposite materials.

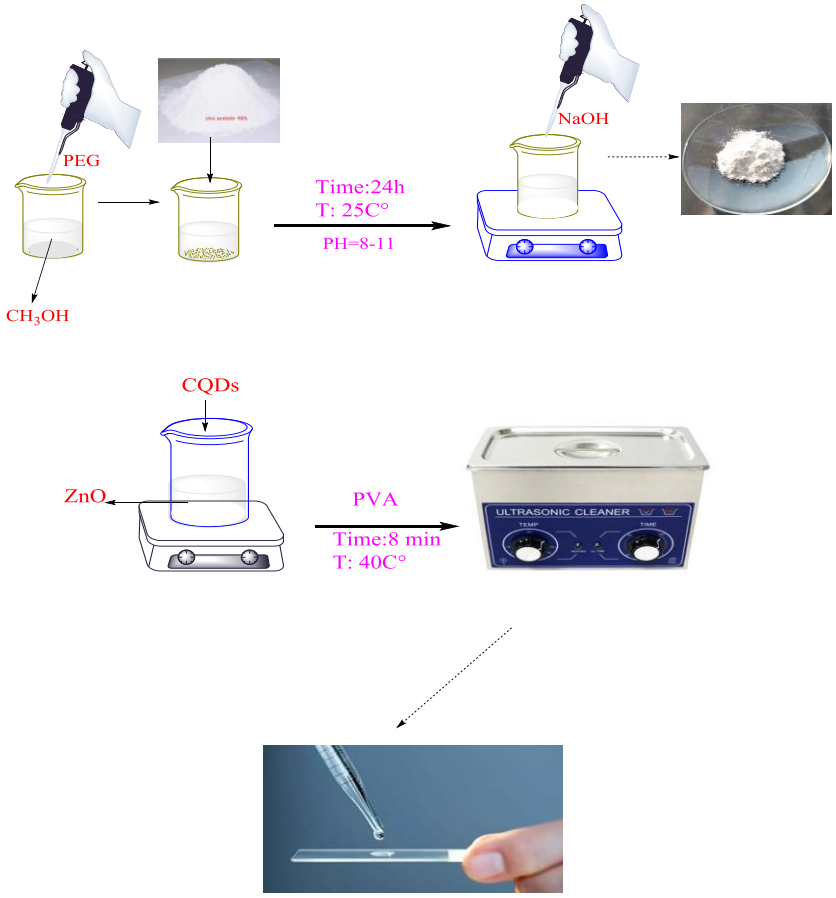

Fig. 1. General route for the preparation of zinc oxide/carbon quantum dot composite on polyvinyl alcohol substrate

3. Results and discussion

3.1. Characterization data and structural and optical properties of ZnO-CQDs/PVA

Polymer nanocomposites composed of polyvinyl alcohol (PVA) and zinc oxide nanoparticles doped with carbon quantum dots (ZnO/CQDs) were synthesized, and their physical properties were analyzed. In this study, zinc oxide (ZnO) nanoparticles with modified surfaces were prepared and subsequently doped with carbon quantum dots (CQDs). A polymer nanocomposite (ZnO-CQDs/PVA) was then formed. Different concentrations of carbon quantum dots (CQDs) were used while maintaining a constant concentration of 0.1 M zinc oxide nanoparticles (ZnO) in the polyvinyl alcohol (PVA) substrate.

The mixture was heated in a methanol solvent for 10 minutes. The resulting mixture was poured onto glass slides and allowed to dry at room temperature. Finally, the structural properties, morphology, and optical transparency of the nanocomposite layers were investigated. The morphology and structural properties of ZnO-CQDs/PVA

were analyzed using transmission electron microscopy (TEM), X-ray diffraction (XRD), dynamic light scattering (DLS), and UV-Vis spectroscopy.

3.2. Identification steps of synthesized samples

Transmission electron microscope (TEM) images were used to analyze the microscopic structural characteristics of ZnO-CQDs. Fig. 2(a) presents a TEM image of a pure ZnO layer prepared using the solution hydrothermal method. Fig. 2(b) illustrates a TEM image of the ZnO nanocomposite integrated with carbon quantum dots (CQDs).
In Fig. 2(b), it is evident that after the addition of carbon quantum dots (CQDs), the surface of the pure ZnO layer becomes rougher and is populated with spherical nanoparticles. The TEM image of these spherical nanoparticles reveals a graphitic layer structure.
The TEM image of the ZnO nanocomposite with carbon quantum dots (Fig. 2(b)) reveals that the nanoparticles are spherical and well-defined, with an average size of approximately 100 nm, as determined by ImageJ software. However, the prepared ZnO-CQDs nanocomposite exhibits an irregular morphology, with ZnO nanoparticles homogeneously dispersed within the nano-carbon quantum dot framework. Fig. 2(b) emphasizes the contrast between the ZnO sample and the ZnO/CQDs, providing compelling evidence for the formation of a heterostructure in the ZnO/CQDs composite.

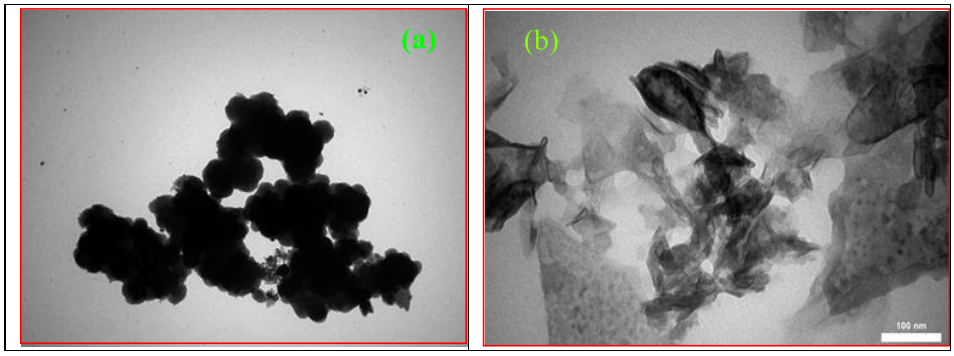

Fig. 2. TEM images of zinc oxide nanoparticle: (a) zinc oxide-carbon quantum dot nanocomposite (b).

Fig. 3 displays the results of dynamic light scattering (DLS) analysis conducted on zinc oxide nanoparticles immediately after synthesis. The size distribution curve generated from the particles indicates the formation of nanoparticles with an average size of 73 nm and a relatively narrow distribution width of approximately 150 nm. These results align with the findings from TEM analysis.

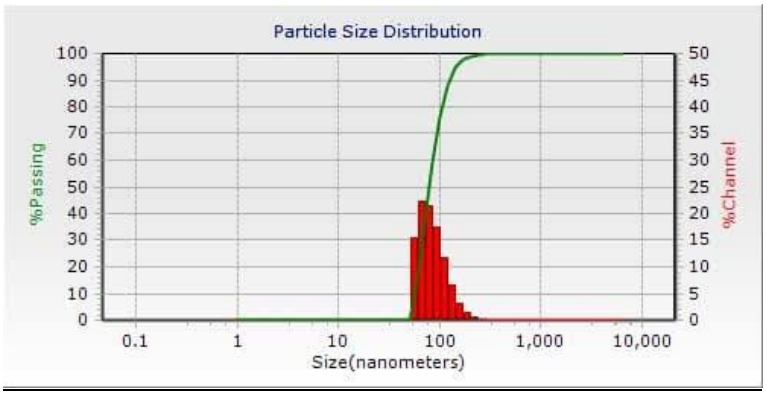

Fig. 3. DLS spectrum of zinc oxide-carbon quantum dot nanocomposite

3.3. Optical studies of zinc oxide/carbon quantum dot nanocomposite with polyvinyl alcohol substrate (ZnO-CQDs/PVA)

The absorption spectrum of a semiconductor directly influences its electronic structure by promoting electron transitions from the valence band to the conduction band through UV-Vis absorption (Akherat Doost et al., 2016, 2021). Fig. 4(A, B and C) depict the electron transition spectra of zinc oxide/carbon quantum dot nanocomposites at concentrations of 1240, 3720, and 2840 µg. The spectra show absorption edges, indicated by dark lines, that extend into the UV region for the zinc oxide/carbon quantum dot nanocomposites. As the wavelength increases, the band gap (E_g) decreases.

The band gap energy of zinc oxide/carbon quantum dot nanocomposites was determined using the Tauc method, which employs the $E_g=(\alpha h\nu)^2/h\nu$. In a typical Tauc plot, the quantity $(\alpha h\nu)^2$ is plotted against hν (light energy), allowing the band gap value of the desired composition to be extracted from the graph (An et al., 2021).

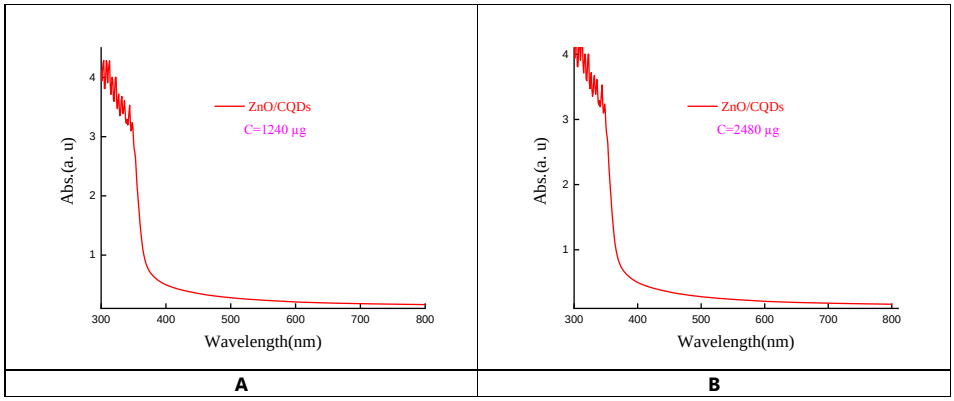

A **B**

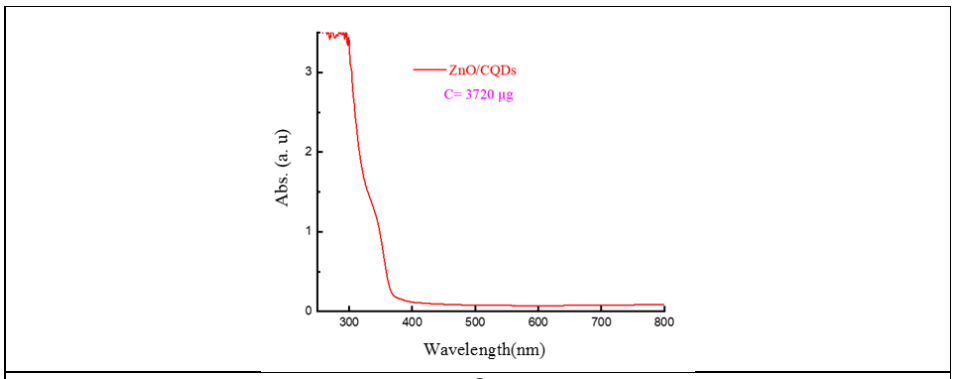

Fig. 4. UV-Vis diagram of zinc oxide/carbon quantum dot nanocomposite at a concentration of **A:** 1240 µg; **B:** 2480 µg and **C:** 3720 µg.

Fig. 5 displays the plot of $(\alpha h\nu)^2$ against photon energy (hν). As depicted in the Fig. 5, the energy gap values obtained at a concentration of 1240 µg of carbon quantum dots illustrate the quantum confinement effects attributable to this concentration level.

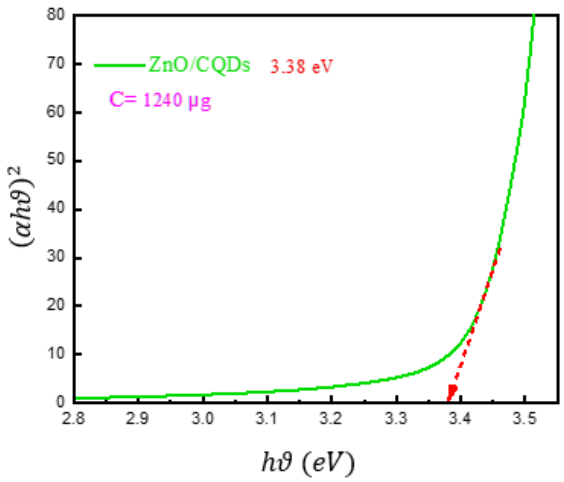

Fig. 5. Graph $(\alpha h\nu)^2$ in terms of photon energy (hν) (eV) of zinc oxide/carbon quantum dot nanocomposite at a concentration of 1240 µg.

Fig. 6 illustrates the plot of $(\alpha h\nu)^2$ as a function of photon energy (hν). As depicted in this figure, the energy gap values obtained at a concentration of 2480 µg of carbon quantum dots are influenced by the quantum confinement effects associated with this concentration level.

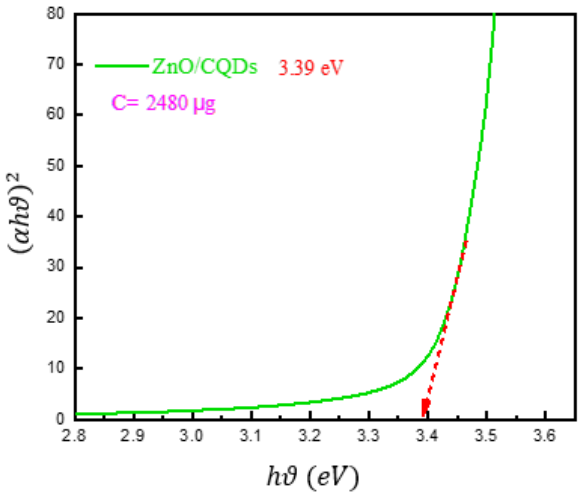

Fig. 6. Graph $(\alpha h\nu)^2$ in terms of photon energy (hν) (eV) of zinc oxide/carbon quantum dot nanocomposite at a concentration of 2480 µg.

Fig. 7 depicts the plot of $(\alpha h\nu)^2$ as a function of photon energy (hν). As observed in this figure, the energy gap values obtained at the concentration of 3720 micrograms of carbon quantum dots reflect the quantum confinement effects influenced by this concentration level. According to Fig. 5, Fig. 6 and Fig. 7, the energy gap diagrams of quantum dot zinc oxide-carbon nanocomposites with concentrations of 1240, 2840, and 3720 µg, prepared by injection into the polymer solution, demonstrate an increase in the energy gap with higher concentrations of carbon quantum dots. This trend indicates the presence of the Burstein-Moss phenomenon.

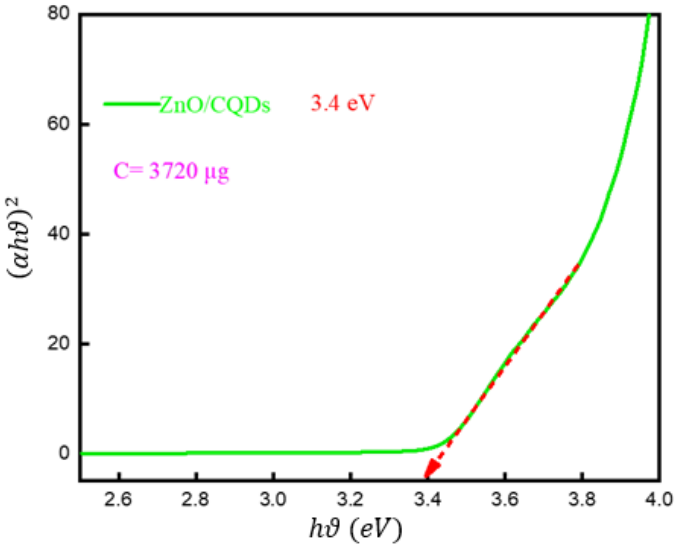

Fig. 7. Graph $(\alpha h\nu)^2$ in terms of photon energy (hν) (eV) of zinc oxide/carbon quantum dot nanocomposite at a concentration of 3720 µg.

Table 1
Energy gap values related to zinc oxide-carbon quantum dot nanocomposite with different concentrations.

Sample	Nano composite type	Concentration (µg)	Energy gap (eV)
1	ZnO-CQDs/PVA	1240	3.38
2	ZnO-CQDs/PVA	2840	3.39
3	ZnO-CQDs/PVA	3720	4
3	PVA	---	---

Based on these measurements, as shown in Table 1, sample 1 corresponds to a zinc oxide-carbon quantum dot nanocomposite with a concentration of 1240 µg, exhibiting an energy gap of 3.38 eV. Sample 2, with a concentration of 2840 µg, demonstrates an energy gap of 3.39 eV. Sample 3, with a concentration of 3720 µg, has an energy gap of 3.4 eV. Therefore, it can be concluded that as the concentration of carbon quantum dots increases, the Burstein-Moss effect becomes more pronounced, resulting in a higher energy gap.

4. Concluding remarks

In the analysis of the energy gap states of zinc oxide, three phenomena are observed: Quantum confinement and two additional phenomena related to the contamination of this material. Quantum confinement is associated with the size of nanoparticles, while contamination results in an increase in carrier density and the introduction of defects, such as impurity atom intercalation, edge dislocations, internal atom intercalation, vacancies, deposition of impurity atoms, continuous displacement due to vacancies, continuous displacement due to intercalation, and replacement of impurity atoms. These defects are commonly referred to as traps.
With zinc oxide contamination, the concentration of impurity atoms increases. Consequently, the Fermi energy for n-type impurities shifts into the conduction band, while for p-type impurities, it shifts into the valence band. This shift results in filled states that inhibit thermal or optical excitations, causing the measured band gap to shift

to higher energies, a phenomenon known as the Burstein-Moss effect, which suppresses low-energy states. In fact, the band gap is determined by the difference between the Fermi energy levels in the conduction and valence bands.
According to the determination of the bandgap in a zinc oxide-carbon quantum dot nanocomposite embedded in a polyvinyl alcohol substrate with varying concentrations of carbon quantum dots, a summary of the optical properties of this nanocomposite is presented below.
The energy gap of the zinc oxide-carbon quantum dot nanocomposite, with concentrations of 1240, 3720, and 2840 µg, was calculated by incorporating it into the polymer solution, resulting in values of 3.38, 3.39, and 3.40 eV, respectively. Furthermore, calculations related to the band gap measurement indicate that as the concentration of carbon quantum dots in the zinc oxide-carbon quantum dot nanocomposite increases, the energy gap also increases, demonstrating the Burstein-Moss phenomenon.

Author contribution statement

Conceptualization and literature search were performed by Hamid Akherat Doost and Ehsan Koushki. The first draft of the manuscript was prepared by Hamid Akherat Doost. Sedighe Zaheri and Reza Tayebee critically analyzed and gave suggestions to finalize the manuscript. All authors read and approved the final manuscript.

Commented [a2]: This section should be added by did the authors in the revision according to the following phrase as a template.
Conceptualization and literature search were performed by Dhananjay Singh and Nishu Mittal. The first draft of the manuscript was prepared by Dhananjay Singh. Nishu Mittal and Mohd Haris Siddiqui critically analyzed and gave suggestions to finalize the manuscript. All authors read and approved the final manuscript.

Conflict of interest

The authors declare that there is no conflict of interest.

References

Akherat Doost, H., Ghasedi, A., Koushki, E., 2021. Electrical effects of AuNPs and PVA polymers on optical band gap and thermo-optical properties of TiO_2 nanoparticles. J. Mol. Liq. 323, 115074.
Akherat Doost, H., Majles Ara, M.H., Koushki, E., 2016. Synthesis and complete Mie analysis of different sizes of TiO_2 nanoparticles. Optik 127(4), 1946-1951.
Alim, M.A., Li, S., Liu, F., Cheng, P., 2006. Electrical barriers in the ZnO varistor grain boundaries. Phys. Status Solidi A 203(2), 410-427.
An, S., Joshi, B. N., Lee, M.W., Kim, N.Y., Yoon, S.S., 2014. Electrospun graphene-ZnO nanofiber mats for photocatalysis applications. Appl. Surf. Sci. 294, 24-28.
Aranovich, J.A., Golmayo, D., Fahrenbruch, A.L., Bube, R.H.,1980. Photovoltaic properties of ZnO/CdTe heterojunctions prepared by spray pyrolysis. J. Appl. Phys. 51(8), 4260-4268.
Bacaksiz, E., Parlak, M., Tomakin, M., Özçelik, A., Karakız, M., Altunbaş, M., 2008. The effects of zinc nitrate, zinc acetate and zinc chloride precursors on investigation of structural and optical properties of ZnO thin films. J. Alloys Compd. 466(1-2), 447-450.
Baedi, J., Ghasedi, A., Koushki, E., Akrami, B., 2021. Nonlinear response of sodium and potassium doped ZnO along with improvement in bandgap structure: A combined physicochemical study. Physica B Condens. Matter 620, 413279.
Berggren, K.-F., Martino, F.,1971. On the calculation of the compton profile in crystalline LiH. Phys. Rev. B, 3(4), 1509-1511.
Burstein, E., 1954. Anomalous Optical Absorption Limit in InSb. Phys. Rev. 93(3), 632-633.
Chang, J.F., Shen, C.C., Hon, M.H., 2003. Growth characteristics and residual stress of RF magnetron sputtered ZnO:Al films. Ceram. Int. 29(3), 245-250.
Chang, S.J., Su, Y.K., Shei, Y.P.,1995. High quality ZnO thin films on InP substrates prepared by radio frequency magnetron sputtering. II. Surface acoustic wave device fabrication. J. Vac. Sci. Technol. A: Vac. Surf. Films 13(2), 385-388.

Gao, C., Zhong, K., Fang, X., Fang, D., Zhao, H., Wang, D., Li, B., Zhai, Y., Chu, X., Li, J., Wang, X., 2021. Brief Review of photocatalysis and photoresponse properties of ZnO-graphene nanocomposites. Energies 14(19), 6403.
Hartnagel, H., 1995. Semiconducting Transparent Thin Films. Taylor & Francis.
Jalili, Z., Koushki, E., Ehsanian, A.H., Tayebee, R., Maleki, B., 2023. Synthesis, band gap structure and third order non-linear optical properties of zinc tungsten oxide nanocomposite using a single CW laser beam. Front. Chem. 11.
Jia, X., Li, J., Wang, E., 2012. One-pot green synthesis of optically pH-sensitive carbon dots with upconversion luminescence. Nanoscale 4(18), 5572.
Khaled, K., Berardi, U., 2021. Current and future coating technologies for architectural glazing applications. Energy Build. 244, 111022.
Koushki, E., Majles Ara, M.H., Mousavi, S.H., Haratizadeh, H., 2011. Temperature effect on optical properties of colloidal ZnO nanoparticles. Curr. Appl. Phys. 11(5), 1164-1167.
Li, H., Kang, Z., Liu, Y., Lee, S.-T. (2012). Carbon nanodots: Synthesis, properties and applications. J. Mater. Chem. 22(46), 24230.
Liu, C., Zhang, P., Zhai, X., Tian, F., Li, W., Yang, J., Liu, Y., Wang, H., Wang, W., Liu, W., 2012. Nano-carrier for gene delivery and bioimaging based on carbon dots with PEI-passivation enhanced fluorescence. Biomaterials 33(13), 3604-3613.
Liu, L., Wang, L., Sun, D., Sun, X., Liu, L., Zhao, W., Tayebee, R., Liu, B., 2023. ZnO-ZnS heterostructure as a potent photocatalyst in the preparation of some substituted chromenes and remarkable antigastrointestinal cancer activity. ACS Omega 8(46), 44276-44286.
Mahan, G.D., 1980. Energy gap in Si and Ge: Impurity dependence. J. Appl. Phys. 51(5), 2634-2646.
Majles Ara, M.H., Akheratdoost, H., Koushki, E. 2015. Self-diffraction and high nonlinear optical properties of carbon nanotubes under CW and pulsed laser illumination. J. Mol. Liq. 206, 4-9.
Nanto, H., Sokooshi, H., Kawai, T., 1993. Aluminum-doped ZnO thin film gas sensor capable of detecting freshness of sea foods. Sensors Actuators B: Chem. 14(1-3), 715-717.
Onodera, A., Takes, M., 2012. Electronic Ferroelectricity in II-VI Semiconductor ZnO. In Advances in Ferroelectrics. InTech.
Sarkar, A., Ghosh, S., Chaudhuri, S., Pal, A.K., 1991. Studies on electron transport properties and the Burstein-Moss shift in indium-doped ZnO films. Thin Solid Films 204(2), 255-264.
Shalahuddin Al Ja'farawy, M., Kusumandari, Purwanto, A., Widiyandari, H., 2022. Carbon quantum dots supported zinc oxide (ZnO/CQDs) efficient photocatalyst for organic pollutant degradation-A systematic review. nviron. Nanotechnol. Monit. Manag. 18, 100681.
Wang, Y., Dong, L., Xiong, R., Hu, A., 2013. Practical access to bandgap-like N-doped carbon dots with dual emission unzipped from PAN@PMMA core-shell nanoparticles. J. Mater. Chem. C 1(46), 7731.
Willander, M., Nur, O., Sadaf, J. R., Qadir, M. I., Zaman, S., Zainelabdin, A., Bano, N., Hussain, I., 2010. Luminescence from Zinc Oxide Nanostructures and Polymers and their Hybrid Devices. Materials *3*(4), 2643-2667.
Xu, X., Chen, Y., Zhang, G., Bian, H., Zhao, M., Ma, S., 2018. Optical properties and the band-gap variation in diverse Zn1-xSnxO nanostructures. Superlattices Microstruct. 123, 349-357.
Zhang, M., Li, J., 2009. Carbon nanotube in different shapes. Mater. Today 12(6), 12-18.
Zhao, Q.-L., Zhang, Z.-L., Huang, B.-H., Peng, J., Zhang, M., Pang, D.-W., 2008. Facile preparation of low cytotoxicity fluorescent carbon nanocrystals by electrooxidation of graphite. Chem. Commun. 41, 5116.